

Polymer Chemistry

Accepted Manuscript



This is an *Accepted Manuscript*, which has been through the Royal Society of Chemistry peer review process and has been accepted for publication.

Accepted Manuscripts are published online shortly after acceptance, before technical editing, formatting and proof reading. Using this free service, authors can make their results available to the community, in citable form, before we publish the edited article. We will replace this *Accepted Manuscript* with the edited and formatted *Advance Article* as soon as it is available.

You can find more information about *Accepted Manuscripts* in the [Information for Authors](#).

Please note that technical editing may introduce minor changes to the text and/or graphics, which may alter content. The journal's standard [Terms & Conditions](#) and the [Ethical guidelines](#) still apply. In no event shall the Royal Society of Chemistry be held responsible for any errors or omissions in this *Accepted Manuscript* or any consequences arising from the use of any information it contains.

Cite this: DOI: 10.1039/c0xx00000x

www.rsc.org/xxxxxx

ARTICLE TYPE

Novel in-situ-foaming materials derived from a naphthalene-based poly(arylene ether ketone) containing thermally labile groups

Duo Qi^a, Chengji Zhao^{*a}, Liyuan Zhang^a, Xuefeng Li^a, Guibin Li^a and Hui Na^{*a}

Received (in XXX, XXX) Xth XXXXXXXXXX 20XX, Accepted Xth XXXXXXXXXX 20XX

DOI: 10.1039/b000000x

A novel in-situ-foaming material was successfully prepared by a naphthalene-based hydroxyl-containing poly(arylene ether ketone) (PAEK) modified with thermally labile *tert*-butyloxycarbonyl which can decompose and in-situ generate CO₂ and isobutene as the foaming agents. The structure and thermal properties of the polymers were characterized by ¹H NMR spectra and thermogravimetry coupled time-resolved mass spectrogram (TG/MS). The resulting polymers exhibited relatively high T_g because of the existence of rigid naphthalene moiety. Then closed microcellular porous membranes with a wide range of expansion ratio (ER) were obtained by a simple thermal treatment from 140 °C to 280 °C for 60 seconds, without using any other physical or chemical foaming agents. The highest ER was 53.98%. This method has never been reported on high-performance poly(aryl ether) materials before. Furthermore, we investigated the relationship between the foaming temperature and the morphology of membranes in detail by density measurement and scanning electron microscope (SEM).

Introduction

Polymeric foams are one important class of lightweight materials because of their high strength to weight ratio, sound and thermal insulation, impact damping^{1,2}. They have been used in a wide variety of applications such as building insulation, transportation, sports equipment, packaging of food, and etc^{3,4}. According to the size of the foam cells, polymer foams can be classified as macrocellular (>100 μm), microcellular (1–100 μm), ultramicrocellular (0.1–1 μm) and nanocellular (0.1–100 nm)⁵. A usual foaming process can be divided into two steps. First, the polymer is saturated under pressure with an inert gas by blowing agents. Then, the pressure is quenched, and the temperature is enhanced to generate porosity in the material^{6–8}. However, the saturation step often needs long time equilibrium and high-pressure devices. Moreover, the widely used physical blowing agent such as supercritical carbon dioxide has low solubility and high diffusivity in polymers which make it difficult to control the foam morphology. Merlet et al.⁹ report a nonconventional foaming process to prepare polymeric foams. Unlike traditional methods, they use gases that generated during the decomposition of side groups on poly(phenylquinoxaline) as foaming agents directly. Nowadays various polymers have been investigated for foam applications, e.g., polyolefin (PE and PP)^{10–15}, polystyrene^{16–19}, polycarbonate^{20–22}, and poly(vinyl chloride)^{23–27}. However, up to now, there is very little research concerned with foam application of high glass transition temperature (T_g) thermoplastics. In addition, most of these studies are focused on the conventional physical foaming process. VanHouten et al.²⁸ used water as a benign blowing agent to produce foam from poly(arylene ether sulfone). Krause et al.²⁹ studied the foaming

behavior of poly(ether imide) and poly(ether sulfone) films using the discontinuous solid-state microcellular foaming process with carbon dioxide as the blowing agent.

Poly(aryl ether ketone)s (PAEKs) are a family of high-temperature engineering thermoplastics with an excellent combination of physical, thermal, and mechanical properties and solvent resistance characteristics. This class of advanced materials is currently receiving considerable attention for potential applications in aerospace, automobile, electronics, and other high technology fields. If combined with foaming technology, one of the greatest merits of PAEK foamed materials is that they can be used at high temperature compared with ordinary polymers. Werner et al. produced carbon nanofiber-reinforced poly(ether ether ketone) foamed materials.³⁰ However, limited studies have been done in this area.

In this paper, we report an elaboration of preparing microcellular foams from a novel PAEK which has never been reported before by in-situ generation of foaming agents. Firstly, we synthesized a novel naphthalene-based poly(arylene ether ketone) containing methoxy groups using 1,5-bis(4-fluorobenzoyl)-2,6-dimethoxynaphthalene (DMNF)³¹ and hydroquinone as monomers. As reported before, the introduction of the rigid planar aromatic structure of naphthalene rings increases the free volume and the stiffness of polymer chains, thus improving their thermal and mechanical stabilities. Then the methoxy groups were converted to the hydroxyl groups, which can easily react with *di-tert*-butyl dicarbonate (Boc₂O). Lastly, we successfully obtained the porous structures by in-situ generation of foaming agents (CO₂ and isobutene) during the thermal treatment of thermo-labile side groups, *tert*-butyloxycarbonyl, i.e., Boc. The structures and properties of these functionalized PAEK polymers containing methoxy, hydroxyl or

Boc groups were characterized in detail, and the characterization of the final porous materials are also presented. Furthermore, we discuss the influence of the thermal treatment temperature on the structures of the PAEK foaming materials.

5 Experimental section

Materials

N-Methyl-2-pyrrolidinone (NMP), *N,N*-dimethylformamide (DMF), *N,N*-dimethylacetamide (DMAc), dimethyl sulfoxide (DMSO) were vacuum-distilled prior to use. Chloroform (CHCl₃), dichloromethane (CH₂Cl₂), toluene, methanol are commercially available grade and used without further purification. 2,6-Dimethoxynaphthalene, 4-fluorobenzoyl Chloride (Sigma-Aldrich Chemical Co.), boron tribromide (BBr₃), ferric chloride (FeCl₃), hydroquinone (Beijing Chemical Reagents), *di-tert*-butyl dicarbonate (Boc₂O), 4-(dimethylamino) pyridine (DMAP) (Aladdin Chemical Co.) were used as received.

Synthesis of monomer 1,5-bis(4-fluorobenzoyl)-2,6-dimethoxy-naphthalene (DMNF)

The synthetic procedure of DMNF has been described in our previous work³¹ (Scheme 1). 2,6-Dimethoxynaphthalene (9.4 g, 0.05 mol) and 4-fluorobenzoyl chloride (17.4 g, 0.11 mol) were dissolved in chloroform. Then anhydrous ferric chloride (1.65 g, 0.01 mol) was added to the mixture at 0-5 °C. And the reaction was then kept at ambient temperature for 24 h. The resulting mixture was poured into hydrochloric acid. The product was removed by decantation and the brown solid was precipitated in methanol. The crude product was then recrystallized from DMF.

Synthesis of naphthalene-based poly(arylene ether ketone) containing methoxy groups (PAEK-OCH₃)

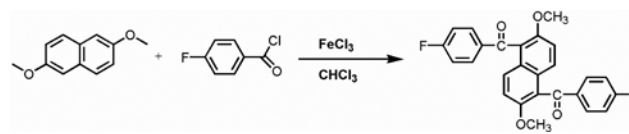
DMNF (4.32 g, 0.01 mol), hydroquinone (1.1 g, 0.01 mol), K₂CO₃ (1.38 g, 0.01 mol), NMP (16 mL) and toluene (10 mL) were added into a 250 mL three-neck flask equipped with a mechanical stirrer, a Dean-Stark trap and a nitrogen inlet/outlet. The mixture was heated at 140 °C for about 2 h to remove water. Then the reaction was allowed to proceed at 180 °C for about 4 h until a highly viscous mixture was obtained. After poured into DI water, the product was washed several times and then dried in vacuum at 100 °C for 24 h (Scheme 2-1).

Synthesis of naphthalene-based poly(arylene ether ketone) containing hydroxyl groups (PAEK-OH)

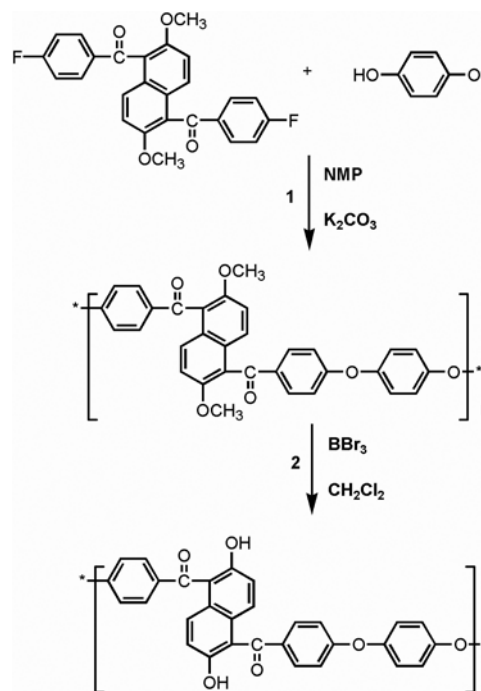
The methoxy groups were converted into hydroxyl according to a modified procedure reported by McOmie et al.³² 1 g PAEK-OCH₃ (3.98 mmol methoxy groups) was dissolved in 10 mL CH₂Cl₂. The solution was cooled down to 0-5 °C (ice bath) and then 1 M solution of BBr₃ in CH₂Cl₂ was added dropwise. The mixture was stirred at room temperature for 6 h before pouring into ice-water to quench excess BBr₃, and then washed with methanol and water. The resulting yellow powder (PAEK-OH) was dried under vacuum at 100 °C for 24 h (Scheme 2-2).

Synthesis of naphthalene-based poly(arylene ether ketone) containing tert-butyloxycarbonyl groups (PAEK-Boc)

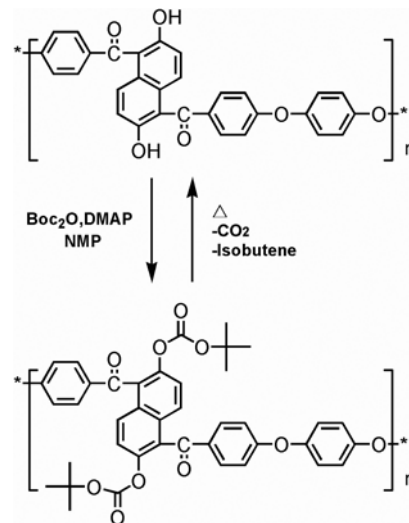
As shown in Scheme 3, PAEK-OH (1 g, 4.21 mmol -OH) was dissolved in 15 mL NMP. Then Boc₂O (1.01 g, 4.63 mmol) was added into the solution. The reaction mixture was stirred at



Scheme 1 Synthesis of monomer DMNF.



Scheme 2 Synthesis of homopolymer PAEK-OCH₃ and PAEK-OH.



Scheme 3 Synthesis of polymer PAEK-Boc.

ambient temperature under a nitrogen flow, and a solution of DMAP (0.035 g, 0.29 mmol) in NMP (2 mL) was added dropwise into the mixture. The solution was stirred an additional 12 h. The resulting polymer (PAEK-Boc) was precipitated in methanol and washed by methanol for several times, and then dried under vacuum at 50 °C overnight.

70 Preparation of the membranes

PAEK-Boc membranes were cast onto the glass plates from their NMP solutions (10 wt.%) and dried at 50 °C for 24 h. The

membranes were then peeled off from the substrates. Subsequently, the dense membranes were immersed in a methanol bath for 24 h to remove the excess solvent, and then dried at 50 °C for another 24 h. The thicknesses of these

5 membranes are $30 \pm 3 \mu\text{m}$.

The resulted PAEK-Boc membranes were then placed in an oven at controlled temperatures (foaming temperature, T_f) for 60 seconds (foaming time) to obtain porous membranes.

Characterizations

^1H NMR spectra were measured on a Bruker Avance 510 spectrometer using $\text{DMSO-}d_6$ or CDCl_3 as the solvent and tetramethylsilane (TMS) as the standard. Fourier transform infrared spectra (FTIR) were recorded on a Bruker Vector-22 spectrometer.

The T_g values of polymers were determined by differential scanning calorimetry (DSC) measurement performed on a TA Instruments DSC Q 20 under nitrogen at heating and cooling rate of $10 \text{ }^\circ\text{C min}^{-1}$ in a temperature range of 50-300 °C. To remove any previous thermal histories, T_g was obtained from the second heating run. The thermal decomposition process of polymers were measured by thermogravimetric analyses (TGA) carried on Pyris1TGA (Perkin Elmer) under flowing nitrogen from room temperature to 800 °C at a heating rate of $20 \text{ }^\circ\text{C min}^{-1}$. Thermogravimetry coupled time-resolved mass spectrogram (TG/MS) (Netzsch STA 449 F3 Jupiter[®]/QMD 403D Aëolos)

was used for further study of the foaming process. The average cell size and cell density were obtained by scanning electron microscopy (SEM) performed on a JEOL JSM-6700F scanning electron microscope. The cross-sectional SEM measurement was performed by fracturing the membrane in the liquid nitrogen and the fractured surface was sputter-coated with Au prior to measurement.

The mass densities of the foamed polymer samples were analyzed by using the flotation weight loss method (DH-3000M) with water as liquid. Water uptake in the foamed sample could not be observed during the measurement, which would overestimate the true density.

The expansion ratio (ER) is defined as the ratio between the density of the initial sample (ρ_s) and that of the foam (ρ_f)³³ and given by Eq.1. The gas volume fraction (V_g) is calculated by Eq.2.

$$\text{ER} = \rho_s / \rho_f \quad \text{Eq.1}$$

$$V_g = 1 - \rho_f / \rho_s \quad \text{Eq.2}$$

The cell nucleation density (N_0) is calculated by the method reported before (Eq.3)³⁴.

$$N_0 = \left(\frac{nM^2}{A} \right)^{\frac{3}{2}} \times \text{ER} \quad \text{Eq.3}$$

In Eq.3, n is the number of cells in the micrograph, M denotes the magnification, A denotes the area of micrograph (cm²), and ER is the expansion ratio.

Results and discussion

Synthesis and characterization of the methoxyl, hydroxyl, and tert-butyloxycarbonyl functionalized homopolymers

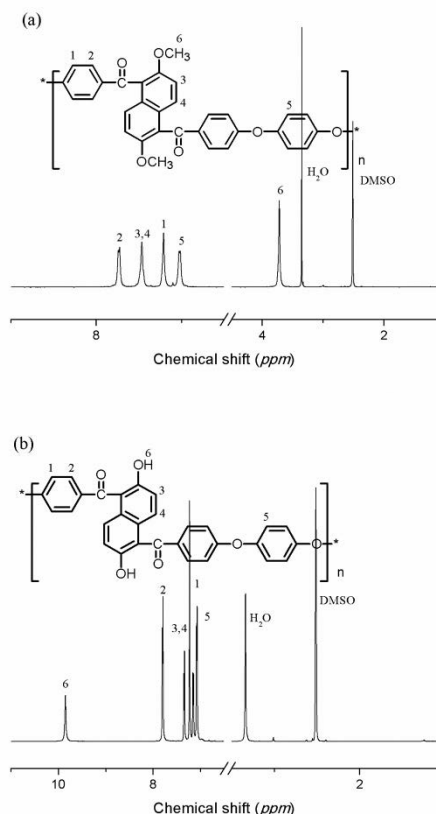


Fig. 1 ^1H NMR spectra of PAEK-OCH₃ (a) and PAEK-OH (b).

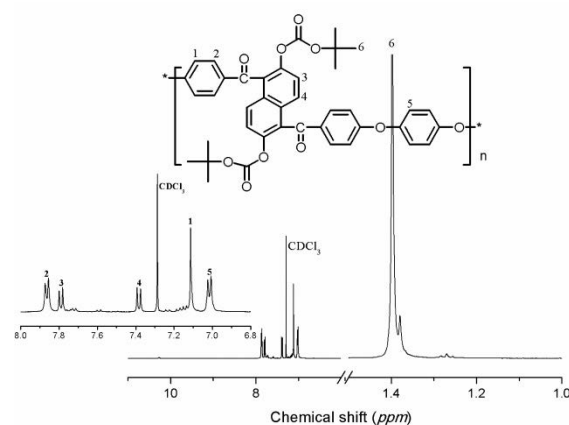


Fig. 2 ^1H NMR spectrum of poly(arylene ether ketone) containing *tert*-butyloxycarbonyl groups (PAEK-Boc).

The PAEK-OCH₃ was synthesized by a nucleophilic substitution polycondensation reaction of DMNF and hydroquinone in NMP, as depicted in Scheme 1. The conversion of methoxyl groups to hydroxyl groups was completed in CH_2Cl_2 using BBr_3 to obtain the PAEK-OH. Fig.1 (a) and (b) show the liquid phase ^1H NMR spectra of PAEK-OCH₃ and PAEK-OH with $\text{DMSO-}d_6$ as the solvent, respectively. The proton peak at $\delta=3.7 \text{ ppm}$ in Fig.1 (a) represented the hydrogen atom of $-\text{OCH}_3$, which disappeared completely in Fig.1 (b). Instead, the characteristic peak for the proton of $-\text{OH}$ was observed in Fig.1 (b) at 9.8 ppm , which

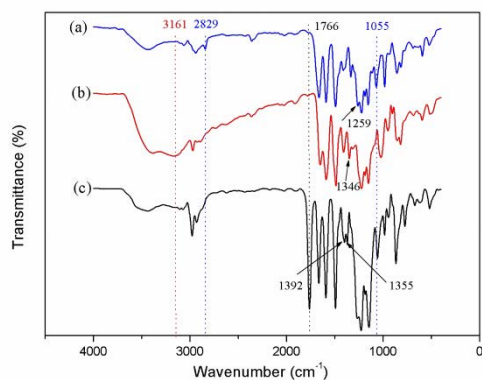


Fig. 3 FTIR spectra of naphthalene-based poly(arylene ether ketone): (a) PAEK-OCH₃, (b) PAEK-OH, (c) PAEK-Boc.

5 indicated that methoxyl groups were converted into hydroxyl groups successfully.

The phenol groups of PAEK-OH were functionalized to *tert*-butyloxycarbonyl groups by reacting with Boc₂O under mild conditions, using DMAP as catalyst.³⁵ Complete Boc grafting was evidenced by ¹H NMR spectrum (Fig.2), using CDCl₃ as the solvent. As shown in Fig.2, the chemical shift from 6.8 ppm to 7.9 ppm can be assigned to the hydrogen atoms on the phenyl rings clearly. An intense proton peak at δ=1.4 ppm belonged to the methyl protons in the *tert*-butyloxycarbonyl groups. And there was no peak at δ=9.8 ppm, which indicated the hydroxyl groups were reacted thoroughly.

The structures of three kinds of homopolymers were also studied by FTIR spectra (Fig.3). The absorption bands observed from 1500 cm⁻¹ to 1650 cm⁻¹ can be attributed to the skeleton vibration of naphthalene rings. In Fig.3 a, the characteristic stretching vibration band at 1055 cm⁻¹ belonged to C-O-Ar. The absorption band at 1259 cm⁻¹ was associated with C-C stretching vibration in the aromatic rings of the methyl β-naphthyl ether. The stretching vibration band of methyl C-H was observed at 2829 cm⁻¹. For PAEK-OH (Fig.3 b), the in-plane bending vibration and the stretching vibration of the hydroxyl was observed at 1346 cm⁻¹ and 3161 cm⁻¹, respectively. A sharp and strong characteristic band at 1766 cm⁻¹ was found in Fig.3 c, which was attributed to the C=O absorption of the Boc group. The peak at 1392 cm⁻¹ corresponded to the bending vibration of C-H, and the one at 1355 cm⁻¹ was assigned to the stretching vibration of C-O-C. These results indicated that three kinds of homopolymers containing methoxyl, hydroxyl and Boc groups were successfully synthesized.

Fig.4 shows the thermal induced phase transition behavior of these polymers examined by DSC. The T_g values of these three homopolymers were all above 200 °C, which was much higher than that of traditional bisphenol A type PEEK (T_g: 149 °C)³⁶. It proved that the introduction of naphthalene rings can improve T_g significantly. The T_g of PAEK-OCH₃ was a little higher than that of PAEK-OH because of the steric effect of methoxy groups. The side group of PAEK-OCH₃ (Fig.4 a) was larger than -OH of PAEK-OH (Fig.4 b), thus restricting the segmental motion of the polymer. Unfortunately, the exact T_g of PAEK-Boc was impossible to measure. The endothermic peak at about 80 °C in

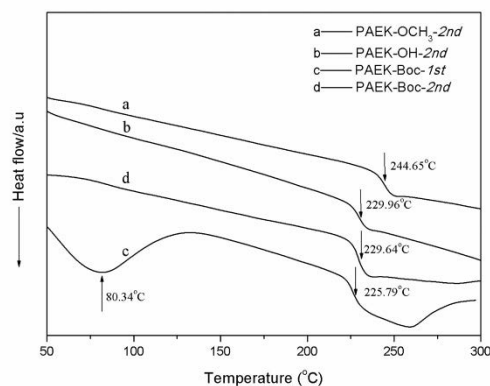


Fig. 4 DSC curves: (a) the 2nd heating procedure of PAEK-OCH₃; (b) the 2nd heating procedure of PAEK-OH; (c) the 1st heating procedure of PAEK-Boc; (d) the 2nd heating procedure of PAEK-Boc.

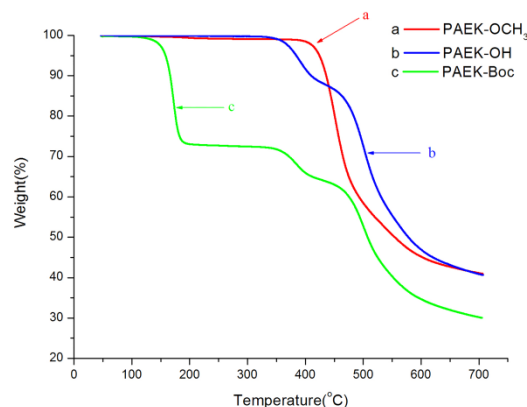


Fig. 5 TGA curves of naphthalene-based poly(arylene ether ketone): (a) PAEK-OCH₃, (b) PAEK-OH, (c) PAEK-Boc

Fig.4 c (the first heating procedure of PAEK-Boc) was associated with decomposition of Boc groups, which was the fundamental cause of foaming. The side groups of PAEK-Boc were then transformed into -OH, so the T_g as showed in Fig.4 d was almost equal to that of PAEK-OH.

The thermal stabilities of the polymers were evaluated by TGA under nitrogen atmosphere (Fig.5). Although the decomposition temperature of PAEK-OCH₃ (380 °C) was higher than PAEK-OH, both PAEK-OCH₃ and PAEK-OH showed excellent thermal stability (decomposition temperature >330 °C). As shown in Fig.5 c, the heat-labile Boc groups started decomposing at about 110 °C, and reached a maximum decomposition temperature at 170 °C. The weight loss was 27.5%, which was in good accordance with the theoretical decomposition (29.2%). After Boc decomposed, *tert*-butyloxycarbonyl-functionalized polymer showed similar TGA curve to that of PAEK-OH. It was attributed to the recovery of the PAEK-OH structure. The details of the decomposition of Boc will be discussed in next section.

The decomposition of PAEK-Boc

To fully understand the process of Boc decomposition reaction, TG/MS spectrogram was shown in Fig.6. More than a simple

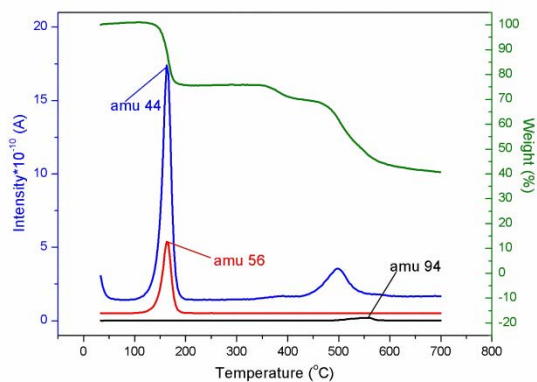


Fig. 6 TG/MS spectrogram of PAEK-Boc.

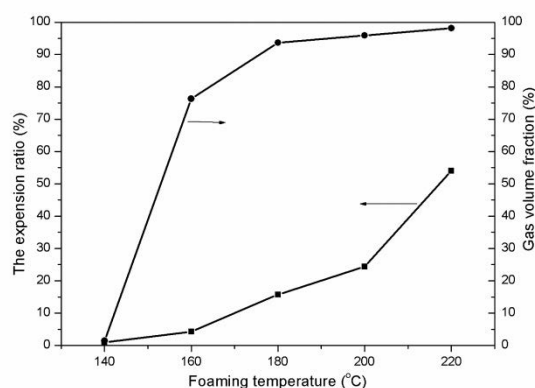


Fig. 7 The dependence relationship of ER and V_g with the foaming temperature.

characterization of the weight loss, the kind of small molecules released during the decomposition process can be detected by TG/MS. The molecular weight of 44 refers to the carbon dioxide, and the substance with a molecular weight of 56 is isobutene. It can be observed distinctly in Fig.6 that both of carbon dioxide and isobutene were simultaneously produced during the decomposition of Boc groups at 170 °C. Moreover, signals of carbon dioxide and molecular weight of 94 appearing in the temperature range of 480 °C-600 °C were associated with CO₂ and carbohydrate generated during the decomposition of polymer main chains.

The expansion ratio and cell nucleation density of the foaming membranes

It has been reported that the decomposition process of Boc was extremely rapid, and could finish in a minute⁹. So in this work we chose 60 seconds as the foaming time. Since ER and N_0 can reflect the situation of nucleary, cell growth and distribution, they are crucial to explore the relationship between the foaming conditions and the cell structures. The calculation methods are given by Eq.1 and Eq.3. There is a wide recognition that the nucleation-growth process occurs at the temperatures above T_g for the polymer/gas mixture³⁷. The CO₂ and isobutene gas dissolving in the polymer matrix act as the plasticizers; as a consequence, they will dramatically reduce T_g of the mixture.^{38,39}

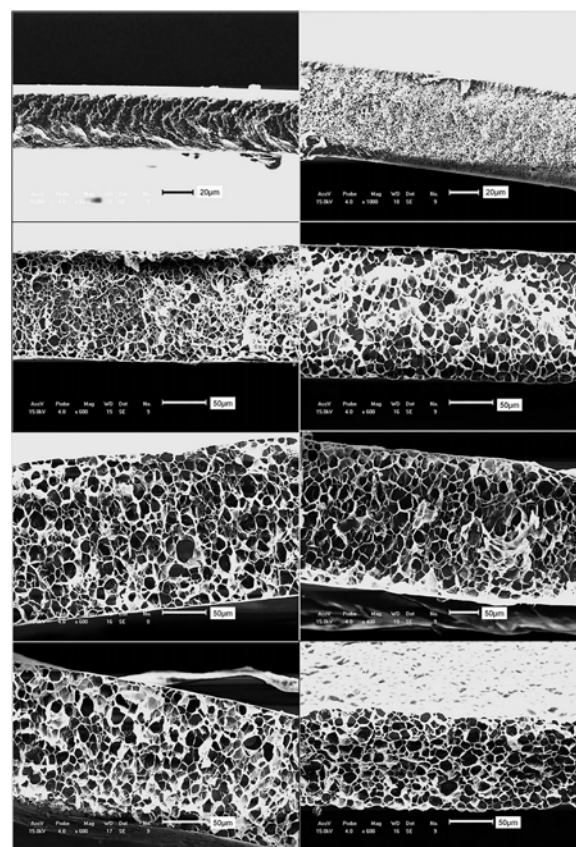


Fig. 8 The cross-sectional SEM images of foamed samples at different T_f at relatively low magnification: (a) 140 °C (b) 160 °C (c) 180 °C (d) 200 °C (e) 220 °C (f) 240 °C (g) 260 °C (h) 280 °C; The white line segment indicates 20 μ m in (a) and (b), and 50 μ m in (c)-(h).

Considering T_g of the homopolymer PAEK-OH (229 °C), we chose the temperature ranging from 140 °C to 220 °C as T_f to study ER and N_0 . The cell properties of foamed membranes are shown in Table 1. There was no significant difference in the mass density and ER after treatment at $T_f=140$ °C. We can infer that 140 °C was not higher than T_g of the polymer/gas mixture. The absence of porous structure can be explained by the glassy state, which hinders the chain mobility at the temperatures below T_g . As the T_f increased from 160 °C to 220 °C, the mass density decreased, while ER and V_g increasing rapidly. Meanwhile, the average cell size increased from 2 μ m to 17 μ m. The phenomenon implied the formation and the growth of cells over 140 °C because of the sufficiently decreasing viscosity and the enhancing chain mobility at higher temperatures. In addition, N_0 decreased with the elevation of T_f , especially from 160 °C to 180 °C. This can be also explained by the chain mobility. The location of gas generation was similar on the polymer chain at different T_f . But as the chain mobility was enhanced, some of the cell walls were destroyed. Then the cells became connected in some degree and N_0 decreased.

Fig.7 reveals the dependence relationship between T_f and cell structure. When T_f increased from 160 °C to 220 °C, V_g increased from 76.32% to 98.15%, and ER had a signally increment from 4.22% to 53.98%. PAEK-Boc was heated transiently, but producing a large amount of gas as the foaming

Table 1 The cell properties of foamed samples

Foaming temperature (°C)	Mass density (g/cm ³)	Expansion ratio (ER) (%)	Gas volume fraction (V _g) (%)	Cell nucleation density (N ₀) (cells/cm ³) ^a	Average cell size (μm) ^b
140	1.2239	1.01	1.42	— ^c	— ^c
160	0.2938	4.22	76.32	1.07×10 ¹¹	2
180	0.0791	15.70	93.63	6.23×10 ⁸	7
200	0.0509	24.39	95.90	4.91×10 ⁸	12
220	0.0230	53.98	98.15	1.03×10 ⁸	17

^a N₀ was obtained from macrograph containing 100-200 cells in Fig.8; ^b cell size was averaged over the measurement of 20 cells in Fig.8; ^c cell structure couldn't be observed in the macrograph. The initial mass density of PAEK-Boc membrane was 1.24 g/cm².

agent because of Boc decomposition. As mentioned before, T_f was higher than T_g of the mixture and the mobility of polymer chain enhanced with T_f increasing. As a consequence, the cell size and ER increased. It is worth to mention that we obtained the controllable closed microcellular structure just by simple thermal treatment. So the nonconventional foaming process by the in-situ generation of foaming agent was convenient and easy to carry out without using physical blowing agent.

The morphology of foamed membranes at different T_f

Fig.8 shows the cross-sectional SEM images of foamed membranes at different T_f. Obviously, the cell structure started to form at 160 °C. Overall, all the membranes presented a closed microcellular structure.

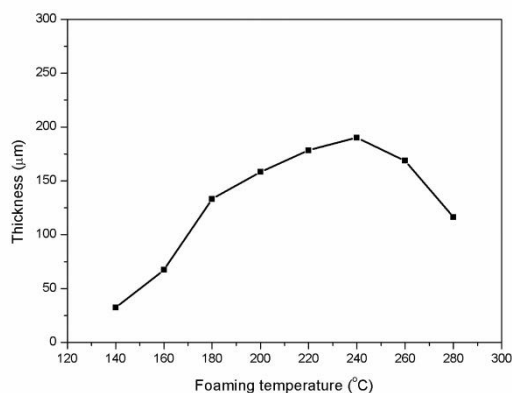


Fig. 9 The thickness of the foamed membrane with the foaming temperature.

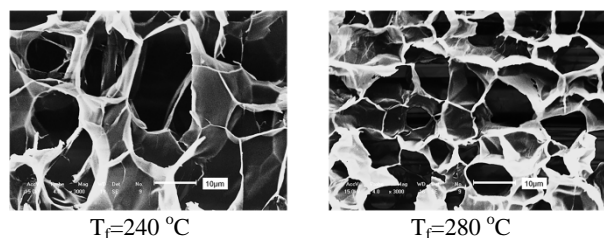


Fig. 10 The SEM micrographs of foamed samples with and without cell collapse; the white line segment indicates 10 μm.

Fig.9 exhibits the relationship between T_f and the thickness of foamed samples. The thickness in Fig.9 was derived from Fig.8 and the value was an average taken from three different positions. The thickness of foamed membrane at 140 °C was 32.5

μm, which was almost the same with that of dense membrane, 30 ± 3 μm. It's moreover interesting to note that with T_f increasing, the thickness of foamed membranes had a peak value of 190.1 μm at 240 °C. And it dropped to 168.7 μm and 116.3 μm at 260 °C and 280 °C, respectively.

The decrease in the thickness at high T_f was caused by pore collapse. As mentioned before, foam formation was driven by gas generated with Boc decomposing. So, T_f should be well controlled to balance the rate of gas evolution and the polymer relaxation; if not, the foam could collapse. As shown in Fig.10, when the cell collapse occurred, the cell size decreased remarkably. Furthermore, there were some defects on the edge of the cells. In the polymer system of this work, the threshold was 240 °C. This can give a general idea of how to choose T_f. And the appropriate range of T_f should be controlled from 160 °C to 240 °C to maintain the intact cell structure.

Conclusions

A new kind of Boc-functionalized in-situ-foaming poly(arylene ether ketone) was successfully obtained by post-modification of a novel hydroxyl-containing PAEK which was synthesized by a polycondensation of DMNF and hydroquinone and following a demethylation reaction. The resulting polymers exhibited high T_g at about 230 °C, because of the existence of naphthalene in the main chain. Closed microcellular structures with a wide range of expansion ratio (from 4.22% to 53.98%) were obtained by adapted thermal treatment of dense polymer membranes. Because of the in-situ generation of CO₂ and isobutene, which were well confirmed by thermal characterization, no other physical or chemical foaming agents were needed. This facile and nonconventional foaming method has never been reported on high-performance polyarylether materials before. We also investigated the relationship between T_f and foaming process. The result showed that T_f was a key parameter to control the cell structure. No porous could be found at a T_f below 140 °C. For 160 °C < T_f < 240 °C, the range of average cell size was from 2 μm to 17 μm. At higher temperature (>260 °C), cell collapse was observed in SEM micrographs.

We think this facile method to prepare high T_g engineering plastic foaming materials has a potential value in many applications such as architecture and aerospace.

Acknowledgement

This work was supported by the National Nature Science Foundation of China (Grant No. 21474036 and 21374034),

Science and Technology Development Plan of Jilin Province (Grant No. 20130522138JH) and the Fok Ying-Tong Education Foundation for Young Teachers in the Higher Education Institutions of China (Grant No. 142010).

5 Notes and references

* Corresponding authors

^aAlan G. MacDiarmid Institute, College of Chemistry, Jilin University, Changchun 130012, PR China. Tel.: +86 431 85168870; Fax: +86 431 85168870 zhaochengji@jlu.edu.cn; huina@jlu.edu.cn

- 10 1. U. Berghaus and R. Wirtz, *Kunststoffe-Plast Europe*, 1999, **89**, 46-+.
2. M. Lee, C. Tzoganakis and C. B. Park, *Advances In Polymer Technology*, 2000, **19**, 300-311.
3. J. Lee, J. Kim, S. W. Kim, C. H. Shin and T. Hyeon, *Chemical Communications*, 2004, 562-563.
- 15 4. N. J. Mills, C. Fitzgerald, A. Gilchrist and R. Verdejo, *Composites Science And Technology*, 2003, **63**, 2389-2400.
5. L. J. Lee, C. C. Zeng, X. Cao, X. M. Han, J. Shen and G. J. Xu, *Composites Science And Technology*, 2005, **65**, 2344-2363.
- 20 6. Park, C. P. *Polymeric Foams; Hanser: New York*, 1991
7. D F Baldwin, C B Park, N P Suh, *Polym Eng Sci*, 1996, **36**, 1425-1435.
8. D F Baldwin, C B Park, N P Suh, *Polym Eng Sci*, 1998, **38**, 674-688.
9. S. Merlet, C. Marestin, F. Schiets, O. Romeyer and R. Mercier, *Macromolecules*, 2007, **40**, 2070-2078.
- 25 10. M. A. Rodriguez-Perez, J. I. Velasco, D. Arencon, O. Almanza and J. A. De Saja, *Journal Of Applied Polymer Science*, 2000, **75**, 156-166.
11. Y. Seo, T. Kang, S. M. Hong and H. J. Choi, *Polymer*, 2007, **48**, 3844-3849.
12. R. W. B. Sharudin and M. Ohshima, *Macromolecular Materials And Engineering*, 2011, **296**, 1046-1054.
- 30 13. W. Zhai and C. B. Park, *Polymer Engineering And Science*, 2011, **51**, 2387-2397.
14. L. Wang, D. Wan, J. Qiu and T. Tang, *Polymer*, 2012, **53**, 4737-4757.
15. G. Zhang, Y. Wang, H. Xing, J. Qiu, J. Gong, K. Yao, H. Tan, Z. Jiang and T. Tang, *Rsc Advances*, 2015, **5**, 27181-27189.
- 35 16. J.-B. Bao, T. Liu, L. Zhao and G.-H. Hu, *Journal Of Supercritical Fluids*, 2011, **55**, 1104-1114.
17. J. Yang, M. Wu, F. Chen, Z. Fei and M. Zhong, *Journal Of Supercritical Fluids*, 2011, **56**, 201-207.
- 40 18. Y. L. Yang and M. C. Gupta, *Nano Letters*, 2005, **5**, 2131-2134.
19. B. Zhu, W. Zha, J. Yang, C. Zhang and L. J. Lee, *Polymer*, 2010, **51**, 2177-2184.
20. G. Gedler, M. Antunes, V. Realinho and J. I. Velasco, *Polymer Degradation And Stability*, 2012, **97**, 1297-1304.
- 45 21. J. W. S. Lee, K. Y. Wang and C. B. Park, *Industrial & Engineering Chemistry Research*, 2005, **44**, 92-99.
22. M. Mitsunaga, Y. Ito, S. S. Ray, M. Okamoto and K. Hironaka, *Macromolecular Materials And Engineering*, 2003, **288**, 543-548.
23. I. Ghasemi, A. T. Farsheh and Z. Masoomi, *Journal Of Vinyl & Additive Technology*, 2012, **18**, 161-167.
- 50 24. R. P. Juntunen, V. Kumar and J. E. Weller, *Journal Of Vinyl & Additive Technology*, 2000, **6**, 93-99.
25. N. Petchwattana and S. Covavisaruch, *Materials & Design*, 2011, **32**, 2844-2850.
- 55 26. Z. Jiang, K. Yao, Z. Du, J. Xue, T. Tang and W. Liu, *Composites Science And Technology*, 2014, **97**, 74-80.
27. K. Yao, H. Tan, Y. Lin, G. Zhang, J. Gong, J. Qiu, T. Tang, H. Na and Z. Jiang, *Rsc Advances*, 2014, **4**, 64053-64060.
28. D. J. VanHouten and D. G. Baird, *Polymer Engineering And Science*, 2009, **49**, 44-51.
- 60 29. B. Krause, H. J. P. Sijbesma, P. Munuklu, N. F. A. van der Vegt and M. Wessling, *Macromolecules*, 2001, **34**, 8792-8801.
30. P. Werner, R. Verdejo, F. Wollecke, V. Altstadt, J. K. W. Sandler and M. S. P. Shaffer, *Advanced Materials*, 2005, **17**, 2864-+
- 65 31. K. Shao, J. Zhu, C. Zhao, X. Li, Z. Cui, Y. Zhang, H. Li, D. Xu, G. Zhang, T. Fu, J. Wu, H. Na and W. Xing, *Journal Of polymer Science Part a-Polymer Chemistry*, 2009, **47**, 5772-5783.
32. McOmie, J.; Watts, D.; West, D, *Tetrahedron*, 1968, **24**, 2289 - 2292.
33. M. Antunes and J. Ignacio Velasco, *Progress In Polymer Science*, 2014, **39**, 486-509.
- 70 34. V. Kumar and J.E. Weller, *SPE ANTEC Tech Papers*, 1991, **37**, 1401.
35. Guibe´-Jampel E and Wakselman M, *Synthesis*, 1977, **11**, 772-773.
36. K. Shao, Naphthalene-based side-chain-type sulfonated poly(arylene ether ketone) copolymers for proton exchange membranes: synthesis and performance studies (in Chinese), Jilin Univ., 2010.
- 75 37. H. E. Naguib, C. B. Park and N. Reichelt, *Journal Of Applied Polymer Science*, 2004, **91**, 2661-2668.
38. A. I. Cooper, *Journal Of Materials Chemistry*, 2000, **10**, 207-234.
39. Y. P. Handa and Z. Y. Zhang, *Journal Of Polymer Science Part B-Polymer Physics*, 2000, **38**, 716-725.
- 80